Chemical Engineering Journal 147 (2009) 188–193

Contents lists available at ScienceDirect

Chemical Engineering Journal

journal homepage: www.elsevier.com/locate/cej

Application of titanate nanotubes for Cu(II) ions adsorptive removal from aqueous solution

Shin-Shou Liu, Chung-Kung Lee*, Huang-Chi Chen, Cheng-Cai Wang, Lain-Chuen Juang

Green Environment R&D Center and Department of Environmental Engineering, Vanung University, Chung-Li 32061, Taiwan, ROC

ARTICLE INFO

Article history:
Received 17 April 2008
Received in revised form 23 June 2008
Accepted 29 June 2008

Keywords:
Titanate nanotubes
Sodium
Copper ions
Cation exchange

ABSTRACT

The potential of adsorptive removal of Cu(II) ions with titanate nanotubes (TNT) was investigated. TNT was prepared via a hydrothermal treatment of TiO_2 powders in a 10 M NaOH solution at 150 °C for 24 h, and subsequently washed with HCl aqueous solution of different concentrations. Effects of the alteration of microstructures of TNT, induced by the acid washing process, on the Cu(II) ions removal performance were discussed. Also examined was the effects of Cu(II) adsorption on the pore structure characteristics of TNT. It was experimentally concluded that if the amount of Na^+ in the TNT was not very low, the TNT might be a good adsorbent for the removal of Cu(II) ions from aqueous solution with the adsorption capacity reaching 120 mg/g. The adsorption mechanisms of Cu(II) ions from aqueous solution onto TNT were examined with the aid of model analyses of the adsorption equilibrium and kinetic data of Cu(II) ions.

1. Introduction

As a result of industrial activities, many heavy metals generate pollution in the environment and result in some serious health problems due to their accumulation in living tissues throughout the food chain [1]. In recent years, an intensive effort to identify methods for their separation and removal from aqueous solutions was taken. There are several methods for removing heavy metal ions from aqueous solution, such as chemical precipitation, membrane filtration, ion exchange, and adsorption. For adsorption process, the application of adsorption technology utilizing commercial activated carbon and different types of ion exchange resins has become known and taken a place as the most effective technologies for the removal of effluents of heavy metal ions [2,3]. However, both activated carbon and ion exchange resins often suffer from high-cost production and regeneration and have encouraged researchers to look for low-cost adsorbing materials [4–6].

Kasuga et al. [7,8] recently reported the preparation of TiO_2-derived nanotubes by hydrothermal treatment of TiO_2 powders in a 10 M NaOH aqueous solution with different reaction temperatures and times. This method does not require any templates, and the prepared nanotubes have a small diameter of ca. 10 nm, and high crystallinity. Moreover, it was found that the microstructures of TNT were easily affected by the synthetic conditions, including such variables as reaction time, acid washing concentration, and calcination temperature [9–17]. Since the TNT derived from the hydrothermal method possesses ion-exchange properties [9,11,14,16,17] and is also characterized by a high specific surface area and pore volume [12], it may offer a special environment for the removal of heavy metal ions through the cation exchange mechanism. Moreover, the above-mentioned hydrothermal method is also a simple, cost-effective, and environmentally friendly technology and can prepare high-yield TNT samples. Therefore, it may be an important task to examine the potential applications of TNT synthesized by the hydrothermal method for heavy metal ions adsorptive removing from aqueous solution.

The objectives of this study are to examine the potential of TNT to remove Cu(II) ions from aqueous solution. The relationship between the alteration in the microstructure of TNT induced by variation of its sodium contents and the change in the Cu(II) removal capacity of TNT is discussed. Effects of Cu(II) adsorption on the pore structure characteristics of TNT are also examined. The thermodynamic and kinetic parameters of the Cu(II) adsorption process are calculated, in order to examine the mechanisms for removing Cu(II) ions from aqueous solution onto TNT.

* Corresponding author. Tel.: +886 34515811/55718; fax: +886 34622232.
E-mail address: anthony@msa.vnu.edu.tw (C.-K. Lee).

1385-8947/$ – see front matter © 2008 Elsevier B.V. All rights reserved.
doi:10.1016/j.cej.2008.06.034

Table 1
Specific surface area, specific pore volume, and average pore diameter for the examined TNT samples [14]

Solid	Na content (wt.%)	BET Surface Area (m^2/g)	Total pore volume (cm^3/g)	Pore diameter (nm)
S-1	≈0	243.3	0.268	10.3
S-2	1.21	357.5	1.575	14.7
S-3	7.23	241.0	1.091	14.7
S-4	7.27	221.8	0.874	13.0
S-5	7.35	248.9	1.090	14.8
Cu^{2+}/S-4	–	216.5	0.754	9.3

2. Materials and methods

2.1. Preparation and characterization of TNT samples

TNT was prepared using a hydrothermal process similar to that described by Kasuga et al. [7,8] The TiO_2 source used for the TNT was commercial-grade TiO_2 powder P25 (Degussa AG, Germany), with a crystalline structure of ca. 20% rutile and ca. 80% anatase and a primary particle size of ca. 30 nm. In a typical preparation, 6 g of the TiO_2 powder were mixed with 120 mL of 10 M NaOH solution, followed by hydrothermal treatment of the mixture at 150 °C in a 200 mL Teflon-lined autoclave for 24 h. After hydrothermal reaction, the precipitate was separated by filtration and washed with the HCl solution and deionized water. It was expected that acid treatment would play an important role in controlling the amount of sodium ions remaining in the TNT. In this study, a series of acid washing concentrations, including 0.1, 0.01, 0.001, 0.0001, and 0.00001N, was used to prepare TNT with distinct residual sodium contents. Firstly, the TNT precipitate was washed twice with 300 mL of deionized water. Then the samples were washed twice with 300 mL of HCl aqueous solution and deionized water. Finally, the samples were immersed in 1000 mL of HCl aqueous solution for 10 h and then washed with 500 mL of deionized water. The amount of residual sodium ions was measured by atomic absorption spectrometry (Z-5000, Hitachi) and was listed in Table 1. For convenience, we denoted the TNT treated with acid concentrations of 0.1, 0.01, 0.001, 0.0001, and 0.00001N as S-1 to S-5, respectively (see Table 1). The acid-washed TNT samples were dried in a vacuum oven at 110 °C for 8 h and stored in glass bottles until used.

Effects of the remnant sodium contents on the microstructures of TNT samples were characterized with transmission electron microscopy (TEM), X-ray diffraction (XRD), and nitrogen adsorption–desorption isotherms and were reported in our previous investigations [14,17]. According to the TEM images of TNT samples, it can be experimentally concluded that when the sodium content is greater than 1.21 wt.% (or the acid washing concentration is smaller than 0.01N), the nanotubular structure can be well-preserved and the morphological characteristics of TNT samples are rather similar. On the other hand, according to the XRD profiles, for S-3 to S-5, a characteristic peak is observed at approximately $2\theta = 10^\circ$, which is considered to correspond to $H_2Ti_3O_7$ or $Na_xH_{2-x}Ti_3O_7$ crystals. Moreover, for S-2, the peak at approximately $2\theta = 10$ becomes diffuse and for S-1, this characteristic peak does not exist; instead a peak corresponding to anatase-type crystal is observed. From both the TEM image and XRD pattern of S-1, it can be concluded that when the sodium content of TNT is approximately 0 wt.% (meaning a nearly complete proton exchange), the nanotubular structure of titanates may be destroyed. The porous structure characteristics, including BET surface area, pore volume, and pore size, obtained from the conventional analysis of the nitrogen adsorption–desorption isotherms were listed in Table 1. As can be seen from Table 1, S-2 (S-1) has the largest (smallest) surface area and pore volume among the examined TNT samples. The sharp decrease in the pore volume of S-1 may be due to the destruction of layered titanate structure, as shown in the disappearance of characteristic peak at approximately $2\theta = 10^\circ$ in the XRD pattern.

2.2. Cu^{2+} removal capacity of TNT samples

Cu(II) ions obtained from the nitrate salt was selected as the adsorbate in order to examine the heavy metal ions removal characteristics of TNT samples with different sodium contents. The degree of removal of Cu(II) ions from aqueous solution onto TNT samples was obtained by the immersion method. For the immersion experiments, 0.1-g-TNT was added into 100 mL of Cu(II) ions aqueous solutions with the desired concentrations (95–200 mg/L). The initial pH value of the solution was adjusted with a NaOH or HCl solution to reach a desirable value. The preliminary experiment revealed that about 1 h was required for the removal process to reach equilibrium, with a reciprocating shaker equipped with a constant temperature controller and a cover to maintain isothermal conditions. The liquid and solid phases were separated by centrifugation at 8000 rpm for 25 min in a Sorvall RC-5C centrifuge. A 15-ml aliquot of the supernatant was taken and analyzed for Cu(II) ions by an atomic absorption spectrometry (Z-5000, Hitachi). The removal capacity of Cu(II) ions was then calculated using the relation $Q = V\Delta C/m$, where V was the volume of the liquid phase, m was the mass of TNT, and ΔC was the difference between the initial and final concentration of Cu(II) ions in aqueous solution, which could be computed simply from the initial and final atomic absorption spectrometry readings. For the kinetics experiments, the Cu(II) ions removal amounts were determined by analyzing the solution at appropriate time intervals. Effects of temperature on the adsorption data were carried out by performing the adsorption experiments at various temperatures (30, 45, and 60 °C).

In this study, the mechanisms for removing Cu(II) ions from aqueous solution onto TNT surfaces were examined. The adsorption equilibrium data were fitted into the model of Langmuir and Freundlich. The Langmuir equation was applicable to homoge-

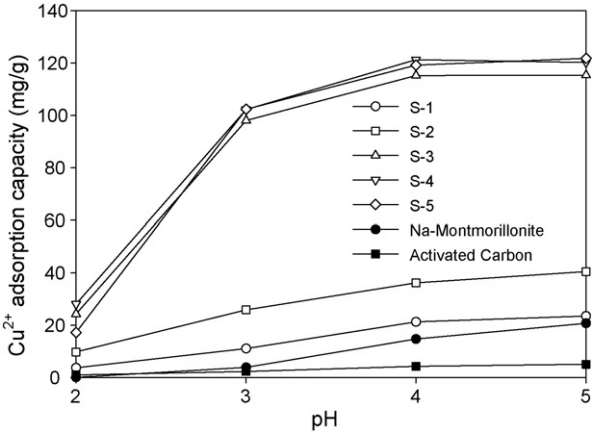

Fig. 1. Effect of pH on the Cu(II) removal capacity of activated carbon, Na-montmorillonite, and TNT samples at 30 °C and initial Cu(II) concentration 200 mg/L.

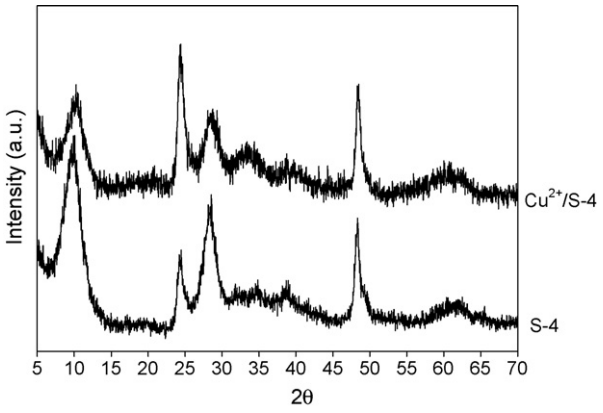

Fig. 2. XRD patterns of S-4 before and after adsorbing Cu(II). *Conditions*: pH 4, 30 °C, and initial Cu(II) concentration 200 mg/L.

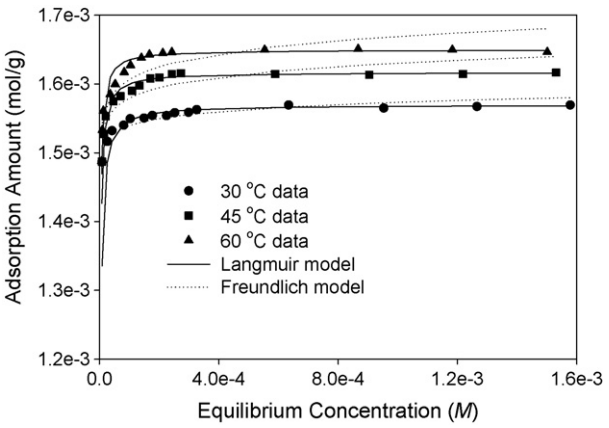

Fig. 4. Langmuir and Freundlich adsorption isotherms of Cu(II) on S-4 at different temperatures and pH 4.

neous adsorption system [18], while the Freundlich equation was an empirical equation employed to describe the heterogeneous systems and was not restricted to the formation of the monolayer [19]. The well known Langmuir equation was represented as

$$\frac{C_e}{Q_e} = \frac{1}{Q_{max}K_L} + \frac{C_e}{Q_{max}}, \quad (1)$$

where Q_e is the equilibrium Cu(II) ions concentration on the adsorbent (mol/g), C_e is the equilibrium Cu(II) ions concentration in solution (mol/L), Q_{max} is the monolayer capacity of TNT samples (mol/g), and K_L is the Langmuir adsorption constant (L/mol) related to the free energy of adsorption. The Langmuir constant K_L is a measure of the affinity between adsorbate and adsorbent and its reciprocal value gives the concentration at which half the maximum adsorption capacity of the adsorbent is reached [18]. A plot of C_e/Q_e versus C_e will give a straight line with slope $1/Q_{max}$ and intercept $1/Q_{max}K_L$ if Langmuir model was held. On the other hand, the Freundlich equation was represented as

$$Q_e = K_F C_e^{1/n}, \quad (2)$$

where K_F (mol/g(L/mol)$^{1/n}$) and $1/n$ are the Freundlich constants corresponding to adsorption capacity and adsorption intensity, respectively [19]. The plot of $\ln Q_e$ versus $\ln C_e$ was employed to generate the intercept K_F and the slope $1/n$.

Moreover, since the adsorption isotherms have been measured at three temperatures, the heat of adsorption can be calculated. The temperature dependency of Langmuir adsorption constant (K_L) obeyed the van't Hoff equation:

$$\frac{d \ln K_L}{dT} = \frac{\Delta H}{RT^2} \quad (3)$$

where R was the gas constant and T was the temperature (in Kelvin). Eq. (3) could be integrated to yield $\ln K_L = \ln K_0 + (-\Delta H/RT)$. A plot of $\ln K_L$ versus $1/T$ will yield a straight line with a slope of $-\Delta H/R$ [20].

For the kinetic data, a simple kinetic analysis was performed with the aid of a pseudo-second-order equation [21]. In this equation, the value of the rate constant k could be calculated with the formula

$$\frac{dQ_t}{dt} = k(Q_s - Q_t)^2 \quad (4)$$

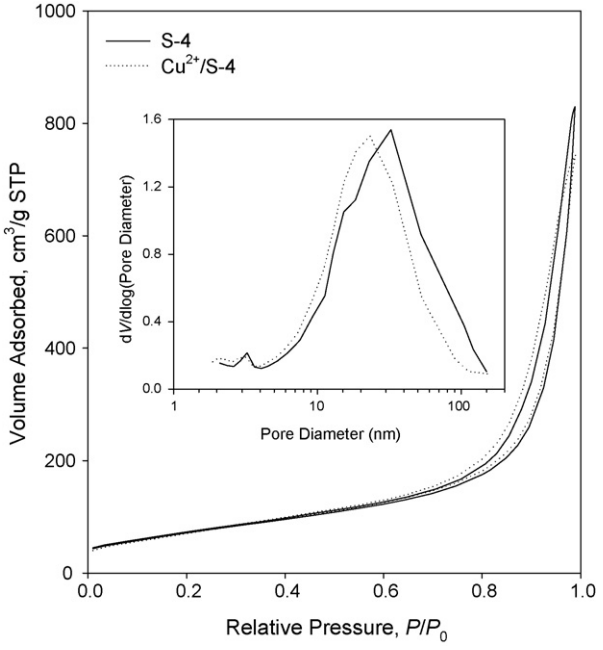

Fig. 3. Nitrogen adsorption–desorption isotherms of S-4 before and after adsorbing Cu(II) and the corresponding pore size distributions (the inserted figure), where V is the cumulative pore volume (cm^3/g).

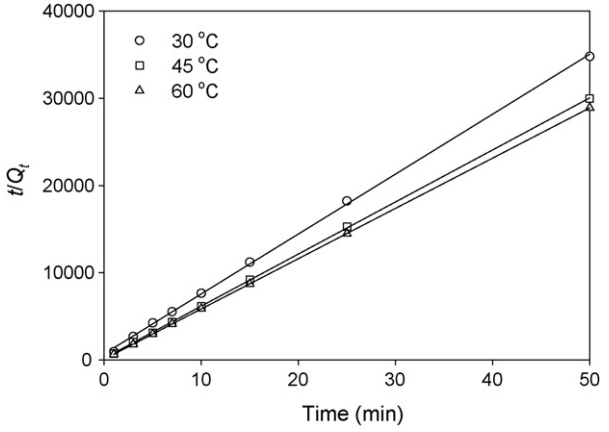

Fig. 5. Comparison of pseudo-second-order kinetics of adsorption of Cu(II) onto S-4 at different temperatures. *Conditions*: initial Cu(II) concentration 200 mg/L and initial pH value of 4.

Table 2
Langmuir and Freundlich isotherm constants for the adsorption of Cu(II) ions onto S-4

T (°C)	Langmuir			Freundlich		
	Q_{max} (mol/g)	K_L (L/mol)	r_L^2	$1/n$	K_F (mol/g(L/mol)$^{1/n}$)	r_F^2
30	1.57×10^{-3}	6.81×10^5	0.999	0.0095	1.68×10^{-3}	0.880
45	1.62×10^{-3}	9.46×10^5	0.999	0.0138	1.79×10^{-3}	0.796
60	1.65×10^{-3}	1.12×10^6	0.999	0.0166	1.87×10^{-3}	0.800

where Q_s and Q_t were the removal amount of Cu(II) ions per unit mass of the adsorbent at equilibrium and time t, respectively. After definite integration by applying the initial conditions $Q_t = 0$ at $t = 0$ and $Q_t = Q_t$ at $t = t$, Eq. (4) became

$$\frac{t}{Q_t} = \frac{1}{kQ_s^2} + \frac{1}{Q_s}t. \tag{5}$$

In addition to the pseudo-second-order rate equation, the intraparticle diffusion model was commonly used for examining the steps involved during adsorption, described by external mass transfer (boundary layer diffusion) and intraparticle diffusion [22]. The intraparticle diffusion model was expressed as

$$Q_t = k_d t^{1/2} \tag{6}$$

where k_d was the diffusion coefficient. If the double nature of the intraparticle diffusion plot confirmed the presence of a boundary-layer effect and pore diffusion, the kinetic data could be further analyzed using the Boyd kinetic expression (Eq. (7)) to determine the actual rate-controlling step involved in the Cu(II) ions removal process [23]

$$G = 1 - \frac{6}{\pi^2}\exp(-Bt), \tag{7}$$

$$B = \frac{\pi D}{r^2} = \text{time constant} \tag{8}$$

where D was the effective diffusion coefficient of adsorbate in the adsorbent phase, r was the radius of the adsorbent particles assumed to be spherical, and G was the fraction of solute removed at different times t and given by

$$G = \frac{Q_t}{Q_s} \tag{9}$$

where Q_t and Q_s represented the removal amount (mol/g) at time t and infinite time, respectively. Here we took the Q_s from the pseudo-second-order kinetic model. Substituting Eq. (9) into Eq. (7), the kinetic expression became

$$Bt = -0.4977 - \ln\left(1 - \frac{Q_t}{Q_s}\right). \tag{10}$$

In general, if the plot of Bt versus t was a straight line passing through the origin, the adsorption was governed by a particle-diffusion mechanism; otherwise it was governed by film diffusion [24].

3. Results and discussion

3.1. Effects of pH on the removal of Cu(II) ions with TNT samples

The pH value of the aqueous solution has been identified as the most important variable governing the heavy metal ions adsorption on adsorbent. This is partly because hydrogen ions themselves are strongly competing with heavy metal ions for the adsorption sites. Fig. 1 demonstrates the effect of pH on the removal of Cu(II) ions onto TNT samples from aqueous solutions. It can be seen from Fig. 1 that the adsorption capacity is low at strong acidic condition (pH 2). After pH 2, uptakes increase sharply up to pH 5 since more Cu(II) ions binding sites could be exposed and carried negative charges, with subsequent attraction of Cu(II) ions with positive charge and adsorption onto the adsorbent surface. This can be well explained by the isoelectric points of the as-synthesized TNT samples. Yu and Zhou [25] reported that the isoelectric points for the as-synthesized TNT samples were at about pH 3. Therefore, TNT is negatively charged particles at pH above 3 and Cu(II) ions can be easily adsorbed on the surface of TNT. Experiments are carried out with the pH values of up to 5 due to the fact that copper precipitation appears at higher pH values [26,27].

Fig. 1 also indicates that the Cu(II) ions removal capacity will increase with the increase in the sodium content of TNT samples. The Cu(II) removal capacity of S-1, S-2, S-3, S-4, and S-5 at pH 5 may reach values of 24, 41, 115, 120, and 121 mg/g, respectively. These results indicate that the optimum sodium content in TNT for Cu(II) removal is greater than 7.2 wt.% (or the acid washing concentration is smaller than 0.001N); the Cu(II) removal capacity may arrive at a value of 120 mg/g at pH 5.

In general, the removal of Cu(II) ions with TNT samples is a cation exchange mechanism and the dominating factors controlling the removal capacity are the cation exchange capacity and the pore volume of TNT [14,17]. Since the pore volume of TNT samples may increase with the decrease in the sodium content, the above results imply that the decrease in the amount of Na^+ may also induce a decrease in the cation exchange capacity of TNT samples. However, the low Cu(II) ions removal capacity of S-1 sample is also closely related to its low pore volume, in addition to the decrease in its cation exchange capacity.

As mentioned earlier, activated carbon is often selected as an adsorbent for the adsorptive removal of heavy metal ions from wastewater. On the other hand, montmorillonite is also an ideal adsorbent for the removal of heavy metal ions due to the capability of interlamellar expansion and high cation exchange capacity [28], from which the high amounts of heavy metal ions can be removed by the cation exchange process. TNT also possesses a negative surface charge density but with the incapability of expansion of its nanotubular pore. Therefore, it is an interesting task to compare the removal capacity of heavy metal ions with the activated carbon, montmorillonite, and TNT; in this way the potential of TNT as an adsorbent for the removal of heavy metal ions can also be examined. Effect of pH values on the Cu(II) removal capacity of activated carbon (purchased from Merck) and Na-montmorillonite (SWy-2, purchased from the University of Missouri-Columbia, Source Clay Minerals Repository) at 30 °C are also demonstrated in Fig. 1. As shown in Fig. 1, the Cu(II) adsorption capacities of all TNT samples are higher than that of both activated carbon and Na-montmorillonite, indicating that TNT may be an attractive adsorbent for the removal of heavy metal ions from wastewater.

3.2. Effects of Cu(II) ions adsorption on the microstructure of TNT samples

It is well known that the removal capacity of mesoporous adsorbents for large adsorbates may be closely related to the variation in their pore structure stability during the adsorption process [29]. The XRD patterns accompanied with the Cu(II) adsorption process

are demonstrated in Fig. 2. If the diffraction patterns are compared, it is clearly observed that adsorption process may induce a slight disorder on the layered structure of TNT, as indicated by the weakness of diffraction peak at $2\theta = 10^\circ$. On the other hand, the decrease of titanate interlayer spacing during the adsorption processes is evidenced with the characteristic peak of layered titanate moving to higher angle.

For providing more information about the structure changes of TNT during the copper ions adsorption process, the nitrogen adsorption–desorption isotherms are also measured, as shown in Fig. 3. Some key features may be found directly from this figure. It can be seen that the isotherms of the two TNT samples are type of II (Brunauer's classification [30]) with a broad hysteresis loop at relative pressure (P/P_0) between 0.6 and 1, indicating the presence of mesopores. Furthermore, the isotherm exhibits high adsorption at high relative pressure (P/P_0) range (approaching 1), suggesting the existence of macropores. The shape of the hysteresis loop is of type H3, implying the formation of slitlike pores that are generally associated with aggregates of platelike particles [31]. As for the effects of Cu(II) ions adsorption on the pore structures of TNT, it can be seen that the decrease in the monolayer capacity, thus the BET surface area of TNT, is very slight when Cu(II) ions are adsorbed. Moreover, since the saturation adsorption capacity of nitrogen corresponds to the pore volume of TNT samples, the isotherms shown in Fig. 3 also suggest that the pore volume will decrease as Cu(II) ions are adsorbed onto TNT. Fig. 3 also shows the corresponding pore size distributions of the examined TNT samples. Generally, both TNT samples exhibit bimodal pore size distribution in the mesoporous and macroporous region. It can be seen that Cu(II) ions adsorption process will make a slight change at the smaller pores (<10 nm) and make the pore size distributions at the larger pores (10–100 nm) moving to left, namely, the mean pore size of TNT sample will decrease. Considering the morphology of the titanate samples observed in the TEM images [14,17], the smaller pores (<10 nm) may correspond to the pores inside the TNT and the diameters of these pores are equal to the inner diameter of the nanotubes, while the larger pores (10–100 nm) can be attributed to the voids in the aggregation of the nanotubes. The changes in the porous structure characteristics of S-4 sample after adsorbing Cu(II) ions are listed in Table 1. As shown in Table 1, owing to the adsorption effects of Cu(II) ions, both the mean pore size and pore volume of S-4 sample will decrease.

In follows, the discussion on the adsorption isotherms and kinetics for providing more information about the adsorption mechanism of copper ions onto TNT is given. The work described here will focus on the adsorption of S-4 sample as it possesses the high adsorption capacity of copper ions among the examined TNT samples.

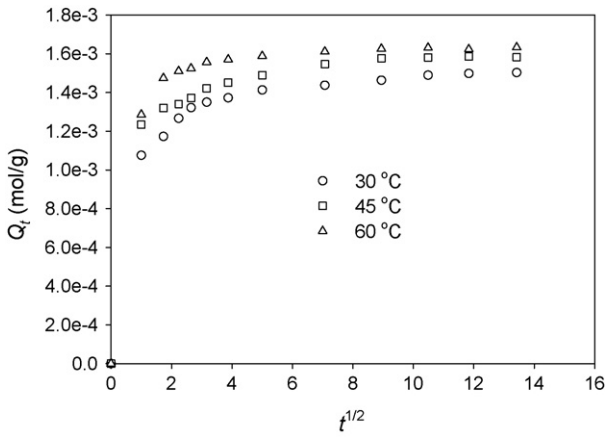

Fig. 6. The diffusion model plots for the adsorption of Cu(II) onto S-4 at different temperatures. *Conditions*: initial Cu(II) concentration 200 mg/L and initial pH value of 4.

Table 3
Parameters of pseudo-second-order model for the adsorption of Cu(II) ions onto S-4

T (°C)	Pseudo-second-order model		
	k (g mol^{-1} min^{-1})	Q_s (mol/g)	R^2
30	6.81×10^2	1.46×10^{-3}	0.999
45	1.90×10^3	1.67×10^{-3}	0.999
60	4.42×10^3	1.73×10^{-3}	0.999

Conditions: initial Cu(II) concentration 200 mg/L and pH value of 4.

3.3. Adsorption isotherms of Cu(II) ions

The equilibrium adsorption isotherm is of importance in the design of adsorption systems. For TNT, its nanotubular structure is assumed to be high degree of pore symmetry and the adsorption environment in TNT may be viewed as a homogeneous system. However, if the adsorption causes a serious disorder in the pore structure of TNT, the adsorption environment may become a heterogeneous system. Accordingly, the equilibrium adsorption data are fitted into the model of Langmuir and Freundlich. The fitting results of both Langmuir and Freundlich models are shown in Fig. 4 and the values of K_L, Q_{max}, K_F, $1/n$, and the linear regression correlations are given in Table 2. As listed in Table 2, Langmuir model should better describe the copper ions adsorption on TNT than Freundlich model. Moreover, the adsorption of copper ions on TNT is largely perceptible to temperature changes, as shown in the variation of both Q_{max} and K_L with temperatures. From the Q_{max}, the adsorption capacities for Cu(II) ions at 30, 45, and 60 °C are 1.57×10^{-3}, 1.62×10^{-3}, and 1.65×10^{-3} mol/g, respectively. On the other hand, the values of $1/n$ are all less than 1 at all temperatures, indicative of high adsorption intensity. If the K_F values are compared at all temperatures studied, it is found that lower values of K_F are obtained at smaller temperatures, indicating that S-4 possesses higher adsorption capacity at higher temperatures.

The increase in Cu(II) ions adsorption capacity of S-4 sample with temperature indicates an endothermic process. The adsorption enthalpy calculated from the van't Hoff equation with the K_L values shown in Table 2 is 14.1 ± 2.1 kJ/mol.

3.4. Adsorption kinetics of Cu(II) ions

The effect of contact time on the amount of Cu(II) ions adsorbed onto S-4 was measured at the optimum initial concentration and different temperatures. A simple kinetic analysis was performed with the aid of pseudo-second-order equation (Eq. (4)). Linear plots of the t/Q_t versus t with linear regression coefficients higher than 0.99 indicates the applicability of this kinetic equation and the pseudo-second nature of the adsorption process of Cu(II) ions onto S-4. Fig. 5 presents the plots for the adsorption of Cu(II) ions on S-4 using the pseudo-second order kinetic model. Table 3 lists the kinetic parameters obtained from the pseudo-second-order model and it is seen that the equilibrium adsorption capacity (Q_s) shows a slight increase with the increasing temperature. From the k values it is observed that for Cu(II) ions, temperature effect on the adsorption kinetics is significant.

In addition to the pseudo-second-order rate equation, the intraparticle diffusion model (Eq. (6)) is also examined. Fig. 6 presents the typical plots for the adsorption of Cu(II) ions on S-4 using the diffusion model. As shown in Fig. 6, the two-phase plot suggests that the adsorption process proceeds by surface adsorption and

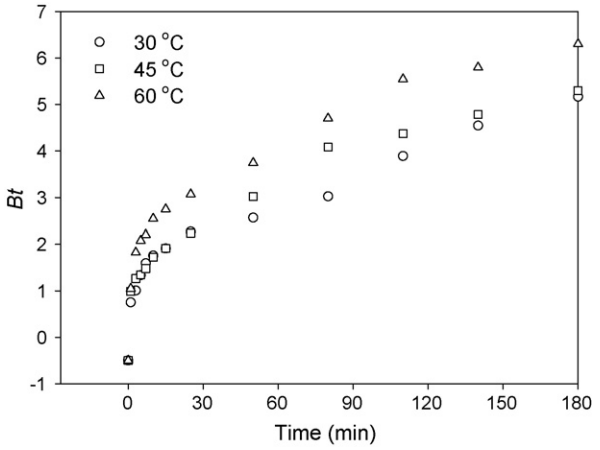

Fig. 7. Correlation between *Bt* and *t* for the adsorption of Cu(II) onto S-4 at different temperatures. *Conditions*: initial Cu(II) concentration 200 mg/L and initial pH value of 4.

intraparticle diffusion, namely, the initial curved portion of the plot indicates a boundary-layer effect while the second linear portion is due to intraparticle or pore diffusion. Because the double nature of intraparticle diffusion plot confirms the presence of a boundary-layer effect and pore diffusion, the adsorption kinetic data can be further analyzed using Boyd kinetic expression (Eq. (7)) to determine the actual rate-controlling step involved in the Cu(II) ions adsorption process. Fig. 7 shows the calculated *Bt* values against *t* for copper ions adsorption at different temperatures. From Fig. 7, it is evident that the plots are not straight lines to pass the origin, implying external mass transport mainly governs the rate-limiting process.

4. Conclusions

It was experimentally concluded that if the sodium content was controlled within an appropriate range (i.e., >7.23 wt.%) and the nanotubular structure of TNT could be well-preserved during the acid washing process, TNT might be an effective adsorbent for the removal of heavy metal ions from aqueous solutions, with the Cu(II) ions removal capacity reaching a value of 120 mg/g at pH 5. The adsorption of Cu(II) may induce a slight disorder on the layered structure of TNT and a decrease in both pore volume and pore size of TNT. The adsorption equilibrium data can be well described with the Langmuir model. Thermodynamic calculations indicated that the adsorption of Cu(II) ions on S-4 might be an endothermic process and the ΔH was 14.1 kJ/mol. The adsorption kinetics followed the pseudo-second-order model and the external diffusion was the controlling process.

References

[1] B. Volesky, Removal and recovery of heavy metals by biosorption, in: B. Volesky (Ed.), Biosorption of Heavy Metals, CRC Press, Boca Raton, FL, 1990, pp. 7–43.
[2] K. Kadirvelu, C. Namasivayam, Activated carbon from coconut coirpith as metal adsorbent: adsorption of Cd(II) from aqueous solution, Adv. Environ. Res. 7 (2003) 471–478.
[3] S. Kocaoba, Comparison of Amberlite IR 120 and dolomite's performances for removal of heavy metals, J. Hazard. Mater. 147 (2007) 488–496.
[4] S.E. Bailey, T.J. Olin, R.M. Bricka, D.D. Adrian, A review of potentially low-cost sorbents for heavy metals, Water Res. 33 (1999) 2469–2479.
[5] Y.H. Wang, S.H. Lin, R.S. Juang, Removal of heavy metal ions from aqueous solutions using various low-cost adsorbents, J. Hazard. Mater. B 102 (2003) 291–302.
[6] S. Babel, T.A. Kurniawan, Low-cost adsorbents for heavy metals uptake from contaminated water: a review, J. Hazard. Mater. 45 (2003) 219–243.
[7] T. Kasuga, M. Hiramatsu, A. Hoson, T. Sekino, K. Niihara, Formation of titanium oxide nanotube, Langmuir 14 (1998) 3160–3163.
[8] T. Kasuga, M. Hiramatsu, A. Hoson, T. Sekino, K. Niihara, Titania nanotubes prepared by chemical processing, Adv. Mater. 11 (1999) 1307–1311.
[9] R. Yoshida, Y. Suzuki, S. Yoshikawa, Effects of synthetic conditions and heat-treatment on the structure of partially ion-exchanged titanate nanotubes, Mater. Chem. Phys. 91 (2005) 409–416.
[10] T. Kasuga, Formation of titanium oxide nanotubes using chemical treatments and their characteristic properties, Thin Solid Films 496 (2006) 141–145.
[11] L.Q. Weng, S.H. Song, S. Hodgson, A. Baker, J. Yu, Synthesis and characterisation of nanotubular titanates and titania, J. Eur. Ceram. Soc. 26 (2006) 1405–1409.
[12] J. Yu, H. Yu, B. Cheng, C. Trapalis, Effects of calcination temperature on the microstructures and photocatalytic activity of titanate nanotubes, J. Mol. Catal. A: Chem. 249 (2006) 135–142.
[13] H. Yu, J. Yu, B. Cheng, M. Zhou, Effects of hydrothermal post-treatment on microstructures and morphology of titanate nanoribbons, J. Solid State Chem. 179 (2006) 349–354.
[14] C.-K. Lee, S.-S. Liu, L.-C. Juang, C.-C. Wang, M.-D. Lyu, S.-H. Hung, Application of titanate nanotubes for dyes adsorptive removal from aqueous solution, J. Hazard. Mater. 148 (2007) 756–760.
[15] C.-K. Lee, C.-C. Wang, M.-D. Lyu, L.-C. Juang, S.-S. Liu, S.-H. Hung, Effects of sodium content and calcination temperature on the morphology, structure, and photocatalytic activity of nanotubular titanates, J. Colloid Interface Sci. 316 (2007) 347–354.
[16] C.-K. Lee, K.-S. Lin, C.-F. Wu, M.-D. Lyu, C.-C. Lo, Effects of synthesis temperature on the microstructures and basic dyes adsorption of titanate nanotubes, J. Hazard. Mater. 150 (2008) 494–503.
[17] C.-K. Lee, C.-C. Wang, L.-C. Juang, M.-D. Lyu, S.-H. Hung, S.-S. Liu, Effects of sodium content on the microstructures and basic dye cation exchange of titanate nanotubes, Coll. Surf. A: Physicochem. Eng. Aspects 317 (2008) 164–173.
[18] I. Langmuir, The adsorption of gases on plane surface of glass, mica and platinum, J. Am. Chem. Soc. 40 (1918) 1361–1368.
[19] H.M.F. Freundlich, Over the adsorption in solution, Z. Phys. Chem. 57 (1906) 385–470.
[20] D.M. Ruthven, Principles of Adsorption and Adsorption Processes, Wiley, New York, 1984, p. 44.
[21] S. Azizian, Kinetic models of sorption: a theoretical analysis, J. Colloid Interface Sci. 276 (2004) 47–52.
[22] S. Wang, H. Li, L. Xu, Application of zeolite MCM-22 for basic dye removal from wastewater, J. Colloid Interface Sci. 295 (2006) 71–78.
[23] G.E. Boyd, A.W. Adamson, L.S. Myers Jr., The exchange adsorption of ions from aqueous solutions by organic zeolites. II: Kinetics, J. Am. Chem. Soc. 69 (1947) 2836–2848.
[24] V. Vadivelan, K.V. Kumar, Equilibrium, kinetics, mechanism, and process design for the sorption of methylene blue onto rice husk, J. Colloid Interface Sci. 286 (2005) 90–100.
[25] J. Yu, M. Zhou, Effects of calcination temperature on microstructures and photocatalytic activity of titanate nanotube films prepared by an EPD method, Nanotechnology 19 (4) (2008) 045606.
[26] P.R. Puranik, K.M. Paknikar, Biosorption of lead and zinc from solutions using *Streptoverticillium cinnamoneum* waste biomass, J. Biotechnol. 55 (1997) 113–124.
[27] H. Niu, X. Shu, J.H. Wang, B. Volesky, Removal of lead from aqueous solutions by *Penicillium* biomass, Biotechnol. Bioeng. 42 (1993) 785–787.
[28] C.C. Wang, L.C. Juang, C.K. Lee, T.C. Hsu, J.F. Lee, H.P. Chao, Effects of exchanged surfactant cations on the pore structure and adsorption characteristics of montmorillonite, J. Colloid Interface Sci. 280 (2004) 27–35.
[29] C.-K. Lee, S.-S. Liu, L.-C. Juang, C.-C. Wang, K.-S. Lin, M.-D. Lyu, Application of MCM-41 for dyes removal from wastewater, J. Hazard. Mater. 147 (2007) 997–1005.
[30] S. Brunauer, The Adsorption of Gases and Vapours, Oxford University Press, 1944.
[31] J. Yu, S. Liu, M. Zhou, Enhanced photocatalytic activity of hollow anatase microspheres by Sn^{4+} incorporation, J. Phys. Chem. C 112 (2008) 2050–2057.